

---

# UAV Path Planning for Maximum-Information Sensing in Spatiotemporal Data Acquisition

---

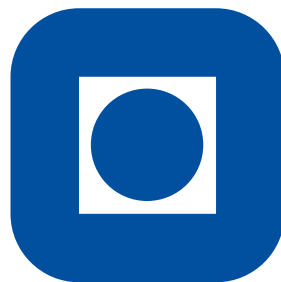
*By:*

**Andreas Nordby Vibeto**

andreanv@stud.ntnu.no

*Supervisor:* **Tor Arne Johansen**

*Co-supervisor:* João F. Fortuna



NTNU

March, 2017

# Contents

<b>1</b>	<b>Introduction</b>	<b>1</b>
1.1	Related Work . . . . .	1
1.2	Hyperspectral Imaging . . . . .	2
1.2.1	Description . . . . .	2
1.2.2	UAV Ground Observation . . . . .	3
<b>2</b>	<b>Theory</b>	<b>4</b>
2.1	Kinematics . . . . .	4
2.1.1	UAV States . . . . .	4
2.1.2	Camera Footprint . . . . .	5
2.2	Optimization . . . . .	6
2.2.1	MPC Method . . . . .	6
2.2.2	Problem Definition . . . . .	6
	<b>Bibliography</b>	<b>8</b>

# Chapter 1

## Introduction

Unmanned Aerial Vehicles (UAV) are today widely used in ground observation, and by equipping them with different sensors they can be used in different situations. While the use of UAV eases many cases of ground observation, there are some difficulties related to the attitude of the aircraft. When the sensor is attached directly to the aircraft the sensor will be coupled with the UAV's states, so that any change in the UAV states will cause a change in what is actually observed by the sensor.

A common solution to decouple the sensor from the UAV states is to attach the sensor to a gimbal which will counteract most of the movements of the UAV. While this is a good solution for decoupling, it raises some new issues regarding its weight and size. As one of the benefits of UAVs is their small size the gimbal can quickly be too big and heavy for the UAV, and it may give less effective aerodynamics. This may again lead to increased fuel consumption for the UAV.

This paper will investigate methods to reduce image errors caused by the UAV's attitude, while also avoiding the extra costs associated with a gimbal. This will be accomplished by optimizing a pre-defined curved path that is to be observed with a model of the UAV. The control method will be developed with a hyperspectral pushbroom camera that is fixed to the UAV in mind.

### 1.1 Related Work

The most common method to decouple the UAV attitude states from the sensor today is to equip the aircraft with a gimbal, which allows "NORMAL" UAV operation without losing track of the features that is to be observed. However, gimbals have limited range and if the UAV angles are too big, the features may be lost from the sensor field of view (FOV). One solution to this problem is to use optimization [1]. Another solution that uses optimization without the use of gimbal is to put constraints on the UAV's roll angle and altitude [2].

A simpler solution to avoid lateral movements of the FOV is to change the UAV course wby using the rudder instead of the ailerons. The rudder deflection creates a yawing moment [3] which causes the aircraft to change course. This type of controller is referred to both as a Rudder Augmented Trajectory Correction (RATC) controller [3] and a skid-to-turn (STT) controller [4]. Results show that the performance of these controllers are comparable to conventional controllers using roll to change course, and that errors in the images is greatly reduced [3] [4] [5].

While the controllers offer a solution to the control problem that reduces the errors in the images, they do not ensure that the ground path that is to be observed will always stay inside the sensors FOV. Optimization is a commonly used method for ensuring that the application succeeds at some "outside" goal, and can be used to e.g. minimize the risk of being identified by radars [6] or plan a path that ensures that a slung load attached to a helicopter do not collide with obstacles [7]. The use of optimization to minimize the error of the sensor footprint for a fixed camera has been done by Jackson [8], by using on-board motion planning.

Jackson presents a path planner that aims to minimize the error between the target on the ground, and the footprint of a camera fixed to a UAV. To achieve this a Nonlinear Model Predictive Controller (NMPC) based on a kinodynamic (an explanation of this would be nice) model of the aircraft is created. The NMPC is compared to a PID and a sliding-mode controller that seek to follow the same path. Simulations of the three controllers show that while the PID controller had much bigger crosstrack errors than the other two, the NMPC and the sliding-mode controller had similar performance. However, the simulations proved that the NMPC controller was able to find a near optimal solution with the performance characteristics of a real-time application.

## **1.2 Hyperspectral Imaging**

The control method developed in this paper will be developed with the use of a fixed hyperspectral, pushbroom sensor in mind. A hyperspectral sensor/camera makes it possible to accurately detect types of material from the UAV by sensing the wavelength of the received light.

### **1.2.1 Description**

Hyperspectral imaging uses basics from spectroscopy to create images, which means that the basis for the images is the emitted or reflected light from materials [9]. The amount of light that is reflected by a material at different wavelengths is determined by several factors, and this makes it possible to distinguish different materials from each other. The reflected light is passed through a grate or a prism that splits the light into different wavelength bands, so that it can be measured by a spectrometer.

When using a hyperspectral camera for ground observation from a UAV, it is very likely that one pixel of the camera covers more than one type of material on the ground.

This means that the observed wavelengths will be influenced by more than one type of material. This is called a composite or mixed spectrum [9], and the spectra of the different materials are combined additively. The combined spectra can be split into the different spectra that it is build up of by noise removal and other statistical methods which will not be covered here.

### **1.2.2 UAV Ground Observation**

Hyperspectral imaging is already being used for ground observation from UAVs. Its ability to distinguish materials based on spectral properties means that it can be used to retrieve information that normal cameras are not able to. For example in agriculture it can be used to map damage to trees caused by bark beetles [10], or it can be used to measure environmental properties, for example chlorophyl fluorescence, on leaf-level in a citrus orchard [11].

Systems for ground observation with hyperspectral cameras can be very complex, which often leads to heavy systems. In [12], a lightweight hyperspectral mapping system was created for the use with octocopters. The purpose of the system is to map agricultural areas using a spectrometer and a photogrammetric camera, and the final "ready-to-fly" weight of the system is 2.0 kg. The resolution of the final images made it possible to gather information on a single-plant basis, and the georeferencing accuracy was off by only a few pixels.

The tests were performed at a low altitude, maximum 120 m. While this was mainly because of local regulations, it also gave a benefit as there was less atmosphere disturbance in the measurements. The UAVs orientation data combined with surface models was used when recovering the positional data in the images. However, they found that externally produced surface models was not accurate enough as they do not take vegetation into consideration. For this reason they supplemented the existing surface models with information gathered during flight.

## Chapter 2

# Theory

### 2.1 Kinematics

When the camera is fixed to the aircraft body, what is actually captured by the camera, the camera footprint, depends on the angles of the aircraft. The equations needed to express the position of the centre and outer points of the camera footprint will be given here. The kinematic model for the UAV used in this paper will also be given here.

#### 2.1.1 UAV States

The position of the UAV will be given using the North East Down (NED) coordinate frame, denoted  $\{n\}$ :

$$\mathbf{p}_{b/n}^n = \begin{bmatrix} N \\ E \\ D \end{bmatrix} = \begin{bmatrix} x_n \\ y_n \\ z_n \end{bmatrix}. \quad (2.1.1)$$

The attitude of the UAV will be given as Euler-angles:

$$\boldsymbol{\Theta}_{nb} = \begin{bmatrix} \phi \\ \theta \\ \psi \end{bmatrix} \quad (2.1.2)$$

with corresponding angular velocities:

$$\dot{\boldsymbol{\Theta}}_{nb} = \begin{bmatrix} p \\ q \\ r \end{bmatrix}. \quad (2.1.3)$$

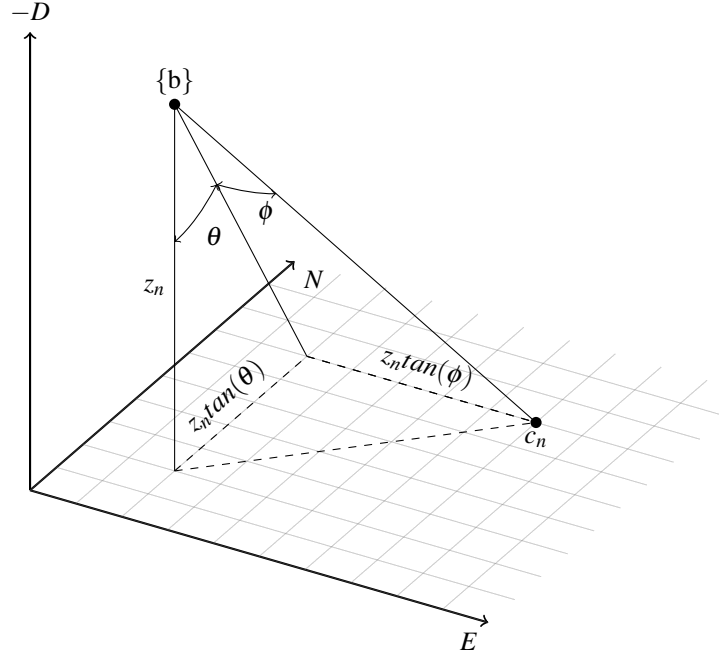


Figure 2.1: Illustration of how the aircraft attitude influence the camera position.

#### ADD WIND KINEMATICS

### 2.1.2 Camera Footprint

The camera footprint is coupled with all of the three angles given in  $\Theta$ . The position of the camera footprint will be calculated using forward kinematics, and the "SITUATION" is shown in figure 2.1.

#### Centre Position

The attitude of the UAV is given in the body frame  $\{b\}$  and the height  $z_n$  is given in the NED frame  $\{n\}$ , and the model assumes flat earth. The position of the footprint centre point  $\mathbf{c}_b^b$  in the body frame  $\{b\}$  is expressed as the geometric (??) distance from the UAV position to the footprint centre point:

$$\mathbf{c}_b^b = \begin{bmatrix} c_{x/b}^b \\ c_{y/b}^b \end{bmatrix} = \begin{bmatrix} z_n \tan(\theta) \\ z_n \tan(\phi) \end{bmatrix}. \quad (2.1.4)$$

The coordinates of the camera position in  $\{n\}$  can be found by rotating the point  $\mathbf{c}_b^b$  with respect to the aircraft heading  $\psi$ , and by translating the rotated point to the aircrafts position in the  $\{n\}$  frame. The rotation matrix for rotating with respect to the heading is given as

$$\mathbf{R}_{z,\psi} = \begin{bmatrix} \cos(\psi) & -\sin(\psi) \\ \sin(\psi) & \cos(\psi) \end{bmatrix}. \quad (2.1.5)$$

The final expression for the camera footprint centre position  $\mathbf{c}^n$  in the  $\{n\}$  frame then becomes:

$$\begin{aligned} \mathbf{c}^n &= \mathbf{p} + \mathbf{R}_{z,\psi} \mathbf{c}_b^b \\ &= \begin{bmatrix} x_n \\ y_n \end{bmatrix} + \mathbf{R}_{z,\psi} \begin{bmatrix} x_{x/b}^b \\ c_{y/b}^b \end{bmatrix} \end{aligned} \quad (2.1.6)$$

### Edge Points

A hyperspectral pushbroom sensor captures images in a line, and the centre point of the camera footprint does not express the entire area that is captured by the sensor. The edge points of the camera footprint are calculated with respect to the sensor's field of view, as shown in figure 2.2. These points  $\mathbf{e}$  can be found by altering 2.1.4:

$$\mathbf{e}_{1,b}^b = \begin{bmatrix} z_n \tan(\theta) \\ z_n \tan(\phi + \sigma) \end{bmatrix}, \quad \mathbf{e}_{2,b}^b = \begin{bmatrix} z_n \tan(\theta) \\ z_n \tan(\phi - \sigma) \end{bmatrix}. \quad (2.1.7)$$

The steps for writing the edge points  $\mathbf{e}$  in the  $\{n\}$  is similar as in equation 2.1.6:

$$\mathbf{e}^n = \mathbf{p} + \mathbf{R}_{z,\psi} \mathbf{e}_b^b. \quad (2.1.8)$$

## 2.2 Optimization

### 2.2.1 MPC Method

### 2.2.2 Problem Definition



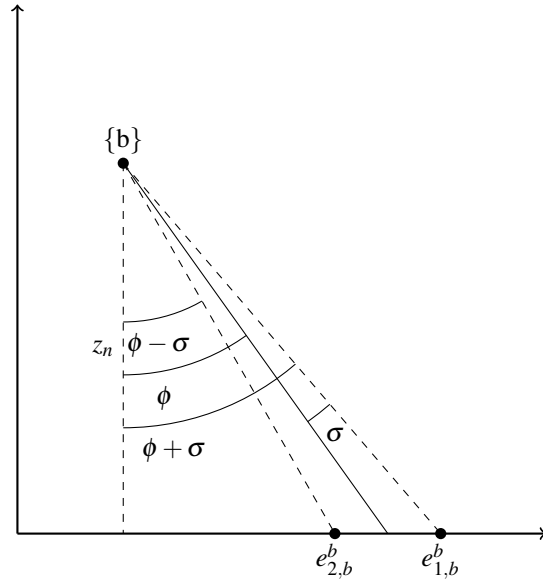


Figure 2.2: Illustration of how the field of view for a pushbroom sensor is calculated.

# Bibliography

- [1] E. Skjong, S. A. Nundal, F. S. Leira, and T. A. Johansen. 2015 international conference on unmanned aircraft systems (icuas). In *Autonomous Search and Tracking of Objects Using Model Predictive Control of Unmanned Aerial Vehicle and Gimbal: Hardware-in-the-loop Simulation of Payload and Avionics*, Denver, Colorado, USA, June 2015. IEEE.
- [2] J. Egbert and R. W. Beard. Proceedings of the 2007 American control conference. In *Low Altitude Road Following Constraints Using Strap-Down EO Cameras on Miniature Air Vehicles*, New York City, USA, July 2007. IEEE.
- [3] Thomas M. Fisher. Rudder augmented trajectory correction for unmanned aerial vehicles to decrease lateral image errors of fixed camera payloads. *All Graduate Theses and Dissertations*, 2016.
- [4] S. Mills, J. J. Ford, and L. Mejias. Vision based control for fixed wing UAVs inspecting locally linear infrastructure using skid-to-turn maneuvers. *Journal of Intelligent and Robotic Systems*, 61(1):29–42, 2011.
- [5] M. Ahsan, H. Rafique, and Z. Abbas. Multitopic conference (INMIC). In *Heading Control of a Fixed Wing UAV Using Alternate Control Surfaces*. IEEE, December 2012.
- [6] T. Inanc, K. Misovec, and R. M. Murray. 43rd IEEE conference on decision and control. In *Nonlinear Trajectory Generation for Unmanned Air Vehicles with Multiple Radars*, Atlantis, Paradise Island, Bahamas, December 2004. IEEE.
- [7] Anders la Cour-Harbo and Morten Bisgaard. *State-Control Trajectory Generation for Helicopter Slung Load System using Optimal Control*. American Institute of Aeronautics and Astronautics Meeting Papers on Disc. 2009.
- [8] Stephen P. Jackson. Controlling small fixed wing UAVs to optimize image quality from on-board cameras. *ProQuest Dissertations and Theses*, 2011.
- [9] Randall B. Smith. *Introduction to Hyperspectral Imaging*. MicroImages, Inc., 2012.
- [10] R. Näsi, E. Honkavaara, P. Lyytikäinen-Saarenmaa, M. Blomqvist, P. Litkey, T. Hakala, N. Viljanen, T. Kantola, T. Tanhuanpää, and M. Holopainen. Using

- UAV-based photogrammetry and hyperspectral imaging for mapping bark beetle damage at tree-level. *Remote Sensing*, 7(15467-15493), 2015.
- [11] P. J. Zarco-Tejada, V. González-Dugo, and J. A. J. Berni. Fluorescence, temperature and narrow-band indices acquired from a UAV platform for water stress detection using a micro-hyperspectral imager and a thermal camera. *Remote Sensing of Environment*, 117(322-337), 2012.
- [12] J. Suomalainen, N. Anders, S. Iqbal, G. Roerink, J. Franke, P. Wenting, D. Hänniger, H. Bartholomeus, R. Becker, and L. Kooistra. A lightweight hyperspectral mapping system and photogrammetric processing chain for unmanned aerial vehicles. *Remote Sensing*, 6(11013-11030), 2014.